Macromolecules

Article

pubs.acs.org/Macromolecules

Ultrabright Fluorescent Polymeric Nanoparticles Made from a New Family of BODIPY Monomers

Chloé Grazon,[†] Jutta Rieger,[‡,*] Rachel Méallet-Renault,[†] Bernadette Charleux,[§] and Gilles Clavier[†,*]

[†]PPSM, ENS Cachan, CNRS, 61 av Président Wilson, F-94230 Cachan, France

[‡]UPMC Univ Paris 06, Laboratoire de Chimie des Polymères (LCP), UMR 7610 94200 IVRY, France and CNRS, Laboratoire de Chimie des Polymères (LCP), UMR 7610, 94200 IVRY, France

[§]Université Lyon 1, CPE Lyon, CNRS UMR 5265, Université de Lyon, C2P2, Team LCPP Bat 308F, 43 Bd du 11 novembre 1918, 69616 Villeurbanne, France

Supporting Information

ABSTRACT: Four novel BODIPY derivatives (π-) functionalized by different polymerizable groups, styrene (S), phenyl acrylate (PhA), ethyl methacrylate (EtMA) and ethyl acrylate (EtA) have been synthesized. Following a formerly established one-pot RAFT miniemulsion polymerization process (Grazon et al. *Macromol. Rapid Commun.* **2011**, *32*, 699−705), the fluorophores were copolymerized in a controlled way at 2.6 mol % with styrene in water. On the basis of the polymerization-induced self-assembly (PISA) principle, the copolymers assembled during their formation into fluorescent nanoparticles. The distribution of the fluorescent monomers along the polymer backbone was monitored by kinetic studies of the copolymerization reaction. Fluorescent stationary and time-resolved spectroscopy was then performed on both the monomers and the nanoparticles (NPs) and the observed differences are discussed in view of the distribution of the fluorescent monomers in the polymer chain. With two of the novel fluorescent monomers (πS and πPhA), the brightness of the NPs could be significantly improved (by a factor 2) compared to particles comprising the other BODIPY monomers. The obtained particles were 200 to 2000 times brighter than usual quantum dots and 40 to 300 times brighter than most of the fluorescent polymeric nanoparticles reported in the literature.

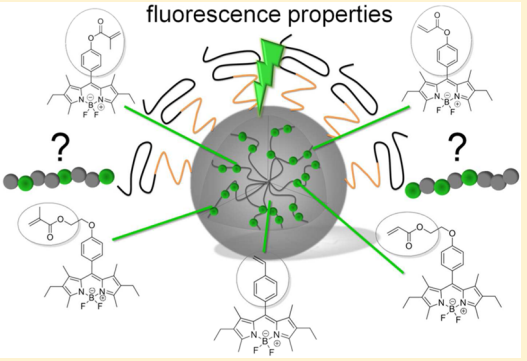

INTRODUCTION

Fluorescent molecules and nano-objects receive nowadays increasing interest for their high potential in sensing, imaging and biomedical applications.[1] Most of the organic fluorophores are hydrophobic compounds that are not soluble in water-based biological media. They can be modified with water solubilizing groups but generally at the expense of the fluorescence quantum yield which drops dramatically.[2] Furthermore, the toxicity of these compounds is not well-known. An appealing alternative is to incorporate them in organic or inorganic (nano)particles that are water-dispersible. However, one of the main problems of this approach is that the fluorophores can leak out of the particles with time. In order to avoid this shortcoming, the best solution is to covalently link the fluorophore to the polymer backbone. This can be achieved either by postmodifying the polymer[3] with reactive fluorophores or by copolymerizing fluorescent monomers with a comonomer. As such, rhodamine,[4] fluorescein[5] or BODIPY-derived monomers[2b] have been successfully used to prepare fluorescent nano-objects. Nevertheless, when fluorophores are concentrated in a confined space such as a particle, luminescence quenching may appear.[6] This usually leads to a decrease in the fluorescence lifetime, quantum yield and therefore the brightness. The latter is a particularly important parameter in the design of fluorescent nanoparticles since it takes into account both absorption and fluorescence parameters and will determine how the fluorescent nano-objects will be detected in single particle fluorescence imaging.

Recent research in controlled radical polymerization (CRP) has shown that atom transfer radical polymerization (ATRP)[7] and reversible addition−fragmentation transfer (RAFT)[8,9] polymerization are efficient tools to achieve polymer chains that are functionalized by fluorescent dyes either at their α-end (using functional initiators)[10] or along the polymer backbone by copolymerization with fluorescent monomers.[11] Indeed, CRP methods are especially appealing compared to conventional radical polymerization since they allow the formation of copolymers which are homogeneous both in molar mass and monomer composition.[12] The microstructure of these copolymers, i.e., the distribution of monomer units within the chain, is governed by the relative reactivity of the monomers M1 and M2, expressed by the reactivity ratios r_{M1} and r_{M2}. Depending on these values as well as on the molar fractions of the

Received: March 20, 2013
Revised: May 28, 2013

   dx.doi.org/10.1021/ma400590q | *Macromolecules* XXXX, XXX, XXX−XXX

monomers in the feed, "random", "gradient", "alternated", or "blocky" structures are obtained.

Hitherto, only few works dealing with the study of the microstructure of fluorescent copolymers have been reported. Winnik et al. have studied the incorporation of fluorescent benzothioxanthene-based monomers possessing a methacrylate function in polymer particles synthesized by emulsion or miniemulsion polymerizations.[13] When copolymerized with styrene or butyl methacrylate as a comonomer, they demonstrated that the fluorescent monomer was homogeneously distributed along the polymer chains. Nevertheless, the fluorescence properties of the obtained nanoparticles were not studied.

We recently reported the synthesis of bright fluorescent nanoparticles with a core made of styrene copolymerized with a BODIPY monomer.[14] BODIPY had been chosen as a hydrophobic fluorophore,[15] as it exhibits attractive spectroscopic characteristics such as an emission spectrum tunable from green to red and high fluorescence quantum yields. The synthesis of the nanoparticles was achieved directly in water by copolymerizing styrene with a few mol % of a phenyl methacrylate BODIPY (πPhMA) derivative in a one-pot RAFT miniemulsion polymerization. This process is very attractive since neither ultrahydrophobic agents nor low molar mass surfactants—which may be detrimental to the targeted biological applications—were used. The stability of the particles and the control of the chain growth were achieved by the use of amphiphilic poly(ethylene oxide)-*block*-poly(acrylic acid)-*block*-polystyrene (PEO-*b*-PAA-*b*-PS) copolymers terminated by a reactive trithiocarbonate RAFT agent, which are chain extended during the miniemulsion polymerization. In a kinetic study of the copolymerization of the BODIPY monomer with styrene, we found that the BODIPY monomer was very rapidly incorporated into the polymer backbone, leading to the formation of a composition gradient of fluorophores. Fluorescence studies showed that the quantum yield of the fluorophore (0.69 in toluene) decreased to 0.20 in the nanoparticles. Parallel research showed that this decrease of the quantum yield was due to poorly fluorescent aggregates of BODIPY, maybe resulting from an inhomogeneous distribution of the fluorescent monomer in the polymer backbone.[16,17] Indeed in the literature, the reactivity ratios r_S and r_{PhMA} for the copolymerization of styrene (S) with phenyl methacrylate (PhMA)—a model monomer for πPhMA—have been reported to be 0.25 and 0.5,[18] respectively, corroborating the initial enrichment of the chains in fluorescent comonomer units.

In this work, we report the synthesis of BODIPY derivatives possessing various polymerizable functions (ethyl acrylate or methacrylate, phenyl acrylate or methacrylate and styrene) and their copolymerization with styrene using the formerly established one-pot miniemulsion polymerization process.[14] The spectroscopic signature of the new BODIPY derivatives was analyzed and compared to that of the particles obtained. The individual consumption of the different monomers was monitored with respect to styrene allowing us to conclude on the microstructure of the copolymers formed. We finally discuss the possibility to establish a relationship between their distribution along the polymer chain and the fluorescence properties of the particles. To the best of our knowledge, this is the first time that such study, namely the attempt to control the distribution of a fluorophore along a copolymer backbone by systematically varying the nature of the polymerizable function, is reported. Previous comparable reports have mainly dealt with the polymerization of different organic fluorophores with the same polymerizable function.[13,19]

EXPERIMENTAL SECTION

Instrumentation. ^{1}H, ^{13}C, ^{11}B, and ^{19}F NMR spectra were recorded in $CDCl_3$ on a JEOL ECS (400 MHz) spectrometer. All chemical shifts are in ppm and referenced to tetramethylsilane (TMS). Coupling constants (J) values are given in Hz. For numbering of protons and carbons in the NMR spectra, see Figure SI-1, Supporting Information.

The number-average molar mass (M_n), the weight-average molar mass (M_w), and the molar mass distribution (polydispersity index M_w/M_n) were determined by size exclusion chromatography (SEC, $M_{n,SEC}$) using THF as an eluent at a flow rate of 1 mL·min^{-1}. For analytical purposes, the acidic functions of the block or alternated copolymers were turned into methyl esters. Therefore, the copolymers were recovered by drying of the aqueous suspensions. After dissolution in a THF/H_2O mixture and acidification of the medium with a 1 M HCl solution, they were methylated using an excess of trimethylsilyldiazomethane.[20] Polymers were analyzed at a concentration of 5 mg·mL^{-1} in THF after filtration through 0.45 μm pore size membrane. The SEC apparatus was equipped with a Viskotek VE 2100 automatic injector and two columns thermostated at 40 °C (PLgel Mixed, 7.5 mm × 300 mm, bead diameter = 5 μm). Detection was made with a differential refractive index detector (Viscotek VE 3580 RI detector) and a UV−vis detector (Waters 486 Tunable Absorbance Detector). The Viscotek OmniSEC software (v 4.6.2) was used for data analysis and the relative M_n and M_w/M_n were calculated with a calibration curve based on polystyrene standards (from Polymer Laboratories).

The z-average particle diameter (named D_z) and the particle size distribution (dispersity factor, named σ), were determined by dynamic light scattering (DLS) of the diluted aqueous dispersions, at an angle of 90° at 20 °C, with a Zetasizer Nano S90 from Malvern, using a 4 mW He−Ne laser at 633 nm. A value of σ below 0.1 is characteristic of a narrow particle size distribution. All calculations were performed using the Nano DTS software.

UV−visible spectra were recorded on a Varian Cary (Palo Alto, CA) double beam spectrometer using a 10 mm path quartz cell from Thuet (Bodelsheim, France). Molar extinction coefficients (ε) are given at the maximal absorption for each monomer, with an error of 5%. Excitation and emission spectra were measured on a SPEX Fluoromax-3 (Horiba Jobin-Yvon). A right-angle configuration was used. Optical density of the samples was checked to be less than 0.1 to avoid reabsorption artifacts. The fluorescence quantum yields Φ_F were determined using Rhodamine 590 (Φ_F = 0.95 in ethanol) as a reference (error of 15%).[21] The fluorescence decay curves were obtained with a time-correlated single-photon-counting method using a titanium-sapphire laser (82 MHz, repetition rate lowered to 4 MHz thanks to a pulse-peaker, 1 ps pulse width, a doubling crystals is used to reach 495 nm excitation) pumped by an argon ion laser from Spectra Physics (Mountain View, CA). For monomers, the Levenberg−Marquardt algorithm was used for nonlinear least-squares fit as implemented in the Globals software (Globals Unlimited, Villa Grove, USA). Lifetimes are given with an error of ±0.05 ns. In order to estimate the quality of the fit, the weighted residuals were calculated. In the case of single photon counting, they are defined as the residuals, i.e., the difference between the measured value and the fit, divided by the square root of the fit. χ^2 is equal to the variance of the weighted residuals. A fit was said appropriate for χ^2 values between 0.8 and 1.2.

For multiexponential fluorescent decays (nanoparticles), no fit was attempted and the average fluorescence lifetimes were calculated by integrating the area below the decay curve as[22]

$$\langle \tau \rangle \equiv \frac{\int_0^\infty tI(t)\,dt}{\int_0^\infty I(t)\,dt} \quad (1)$$

Radiative decay rates (k_r) and non radiative decay rates (k_{nr}) are calculated as:

dx.doi.org/10.1021/ma400590q | Macromolecules XXXX, XXX, XXX−XXX

$$k_r = \frac{\phi_F}{\tau}; \quad k_{nr} = \frac{1-\phi_F}{\tau} \tag{2}$$

Materials. 2,4-Dimethyl-3-ethylpyrrole (97%, Aldrich, kryptopyrrole), boron trifluoride diethyl etherate (2 M in diethyl ether, Aldrich), 4-hydroxybenzaldehyde (98%, Aldrich), tetrachloro-1,4-benzoquinone (99%, Aldrich, Chloranil), *N,N*-diisopropylethylamine (99.5%, Sigma-Aldrich, DIPEA), 1,8-diazobicyclo[5,4,0]undec-7-ene (≥98%, Fluka, DBU), trifluoroacetic acid (99%, Sigma-Aldrich, TFA), acryloyl chloride (97%, Aldrich), triethylamine (≥99%, Sigma-Aldrich), thionyl chloride (99%, Fluka), 4,4′-azobis(4-cyanopentanoic acid) (Aldrich, ACPA), (trimethylsilyl)diazomethane (2 M solution in diethyl ether, Aldrich) were used as received. Solvents (Carlo Erba) were of synthetic grade and purified according to standard procedures. Methacryloyl chloride (97%, Fluka) and styrene were distilled under reduced pressure. 2,2′-Azobis(2-methylpropionitrile) (98%, Sigma, AIBN) was recrystallized from chloroform and few drops of petroleum ether. Silica gel 60 Å (70−200 mm porosity) was bought from SDS.

Synthesis of BODIPY phenol 6: 2,6-Diethyl-4,4-difluoro-8-(4-hydroxyphenyl)-1,3,5,7-tetramethyl-4-bora-3*a*,4*a*-diaza-*s*-indacene. BODIPY phenol **6** was obtained as described elsewhere[23] (6.40 g, yield 80%; ^{1}H NMR (400 MHz, $CDCl_3$) δ = 7.12 (d, 2H, H_{10}), 6.94 (d, 2H, H_{11}), 5.23 (s, 1H, −O*H*), 2.53 (s, 6H, $H_{3'}$, $H_{5'}$), 2.30 (q, 4H, $H_{2'}$, $H_{6'}$), 1.35 (s, 6H, $H_{1'}$, $H_{7'}$), 0.98 (t, 6H, $H_{2''}$, $H_{6''}$); ^{13}C NMR (100 MHz, $CDCl_3$) δ = 156.2, 153.7, 138.6, 132.9, 131.3, 129.9, 128.3, 116.2, 17.2, 14.8, 12.6, 12.0).

Synthesis of Monomer πPhMA 1: 2,6-Diethyl-4,4-difluoro-8-(4-(methacryloyloxy)phenyl)-1,3,5,7-tetramethyl-4-bora-3*a*,4*a*-diaza-*s*-indacene. The synthesis of monomer πPhMA **1** was performed as previously described,[14] by an esterification of BODIPY phenol **6** with methacryloyl chloride (432 mg, yield 78%; ^{1}H NMR (400 MHz, $CDCl_3$) δ = 7.32 (d, 2H, H_{10}), 7.27 (d, 2H, H_{11}), 6.39 (s, 1H, $H_{16'}$), 5.80 (s, 1H, H_{16}), 2.52 (s, 6H, $H_{3'}$, $H_{5'}$), 2.29 (q, 4H, $H_{2'}$, $H_{6'}$), 2.08 (s, 3H, H_{15}), 1.33 (s, 6H, $H_{1'}$, $H_{7'}$), 0.97 (t, 6H, $H_{2''}$, $H_{6''}$) ppm; ^{13}C NMR (100 MHz, $CDCl_3$) δ = 165.69, 154.01, 151.44, 139.22, 138.45, 135.78, 133.32, 133.00, 130.90, 129.53, 127.68, 122.58, 18.46, 17.15, 14.68, 12.60, 11.92 ppm).

Synthesis of Monomer πPhA 2: 2,6-Diethyl-4,4-difluoro-8-(4-(acryloyloxy)phenyl)-1,3,5,7-tetramethyl-4-bora-3*a*,4*a*-diaza-*s*-indacene. The reaction was carried out using the same protocol as for πPhMA **1** using acryloyl chloride to give 565 mg of a pink powder (yield 50%).

^{1}H NMR (400 MHz, $CDCl_3$): δ = 7.33−7.27 (m, 4H, H_{10}, H_{11}), 6.65 (dd, J_{H-H} = 1.2 Hz, J_{H-H} = 17.4 Hz, 1H, H_{15}), 6.36 (dd, J_{H-H} = 17.2 Hz, J_{H-H} = 10.3 Hz, 1H, H_{14}), 6.06 (dd, J_{H-H} =1.2 Hz, J_{H-H} = 10.5 Hz, 1H, H_{15}), 2.53 (s, 6H, $H_{3'}$, $H_{5'}$), 2.30 (q, J_{H-H} = 7.8 Hz, 4H, $H_{2'}$, $H_{6'}$), 1.34 (s, 6H, $H_{1'}$, $H_{7'}$), 0.98 (t, J_{H-H} = 7.3 Hz, 6H, $H_{2''}$, $H_{6''}$) ppm. ^{13}C NMR (100 MHz, $CDCl_3$): δ = 164.3 (C_{13}), 154.0, 151.1, 139.2, 138.4, 133.4, 133.1 (C_{15}), 130.9, 129.5 (C_{10}), 127.8 (C_{14}), 122.4 (C_{11}), 17.2 ($C_{2'}$, $C_{6'}$), 14.7 ($C_{2''}$, $C_{6''}$), 12.6 ($C_{3'}$, $C_{5'}$), 11.9 ($C_{1'}$, $C_{7'}$) ppm. ^{19}F NMR (376 MHz, $CDCl_3$): δ = −145.7 (q, J_{F-B} = 32.3 Hz) ppm. ^{11}B NMR (128 MHz, $CDCl_3$): δ = −0.15 (t, J_{B-F} = 34.5 Hz) ppm. HRMS (ESI) m/z [M + H]$^+$ calculated for $C_{26}H_{29}BF_2N_2O_2H$, 451.2368; found, 451.2359 (100%). Mp =175 °C.

Synthesis of BODIPY πEtOH 7: 2,6-Diethyl-4,4-difluoro-8-(4-(2-hydroxyethoxy)phenyl)-1,3,5,7-tetramethyl-4-bora-3*a*,4*a*-diaza-*s*-indacene. 4-(2-Hydroxyethoxy)benzaldehyde used in this procedure was synthesized according to the literature[24] (325 mg, yield 66%; ^{1}H NMR (400 MHz, $CDCl_3$) δ = 9.90 (s, 1H, *CH*O), 7.85 (d, 2H, J_{H-H} = 8.7 Hz, H_{Ar}), 7.03 (d, 2H, J_{H-H} = 8.7 Hz, H_{Ar}), 4.18 (t, 2H, J_{H-H} = 4.6 Hz, *CH*$_2$), 4.02 (t, 2H, J_{H-H} = 4.6 Hz, *CH*$_2$) ppm).

4-(2-Hydroxyethoxy)benzaldehyde (1 mmol, 0.17 g) and kryptopyrrole (2 equiv., 2 mmol, 0.25 g) dissolved in 25 mL of anhydrous dichloromethane were introduced in a round-bottom flask flushed with argon and equipped with a $CaCl_2$ moisture trap. Then four drops of TFA were added to the reaction. The dark reaction mixture was stirred at room temperature until total disappearance of the aldehyde (determined by TLC analysis). Chloranil (1 equiv, 1 mmol, 0.24 g) was added and the reaction stirred for 2 min. Then DIPEA (7 equiv, 7 mmol, 0.9 g) and boron trifluoride diethyl etherate (11 equiv, 11 mmol, 1.56 g) were introduced. After 2h the reaction was stopped. The mixture was concentrated under vacuum and purified by chromatography on silica gel (dichloromethane, DCM). 318 mg of a pink powder were obtained (yield: 72%).

^{1}H NMR (400 MHz, $CDCl_3$): δ = 7.18 (d, 2H, J_{H-H} = 6.4 Hz, H_{10}), 7.03 (d, 2H, J_{H-H} = 6.9 Hz, H_{11}), 4.16 (t, 2H, J_{H-H} = 4.6 Hz, H_{13}), 4.03 (t, 2H, J_{H-H} = 4.4 Hz, H_{14}), 2.53 (s, 6H, $H_{3'}$, $H_{5'}$), 2.30 (q, 4H, J_{H-H} = 7.6 Hz, $H_{2'}$, $H_{6'}$), 1.33 (s, 6H, $H_{1'}$, $H_{7'}$), 0.98 (t, 6H, J_{H-H} = 7.6 Hz, $H_{2''}$, $H_{6''}$) ppm. ^{13}C NMR (100 MHz, $CDCl_3$): δ = 159.2 (C_{12}), 153.7, 140.2, 138.4, 132.8, 131.3, 129.7 (C_{10}), 128.5, 115.1 (C_{11}), 69.3 (C_{13}), 61.6 (C_{14}), 17.2 ($C_{2'}$, $C_{6'}$), 14.8 ($C_{2''}$, $C_{6''}$), 12.6 ($C_{3'}$, $C_{5'}$), 12.0 ($C_{1'}$, $C_{7'}$) ppm. ^{19}F NMR (376 MHz, $CDCl_3$): δ = −145.7 (q, J_{F-B} = 32.3 Hz) ppm. ^{11}B NMR (128 MHz, $CDCl_3$): δ = −0.15 (t, J_{B-F} = 34.5 Hz) ppm. HRMS (ESI) m/z [M + Na]$^+$ calculated for $C_{25}H_{31}N_2O_2F_2BNa$, 463.2339; found, 463.2342 (100%).

Synthesis of Monomer πEtMA 3: 2,6-Diethyl-4,4-difluoro-8-(4-(2-(methacryloyloxy)ethoxy)phenyl)-1,3,5,7-tetramethyl-4-bora-3*a*,4*a*-diaza-*s*-indacene. BODIPY derivative πEtOH **7** (0.43 mmol, 190 mg) was dissolved in 4 mL of DCM in a round-bottom flask at 0 °C. Once the dye dissolved, triethylamine (7 equiv., 3.0 mmol, 0.41 mL) was added. At last, methacryloyl chloride (1.5 equiv., 65 mmol, 60 μL) diluted in 1 mL of DCM was slowly added to the reaction with a syringe. The reaction was stirred overnight, until disappearance of the πEtOH **7** on a TLC plate. The mixture was then washed twice with ∼50 mL of water and ∼50 mL of brine. The organic phase was dried over $MgSO_4$ and concentrated under vacuum. The residue was purified by chromatography on silica gel (dichloromethane/petroleum ether: 2/1). 100 mg of a pink powder were obtained (yield: 50%).

^{1}H NMR (400 MHz, $CDCl_3$): δ = 7.17 (d, 2H, J_{H-H} = 7.3 Hz, H_{10}), 7.02 (d, 2H, J_{H-H} = 7.3 Hz, H_{11}), 6.19 (s, 1H, H_{18}), 5.62 (s, 1H, $H_{18'}$), 4.54 (t, 2H, J_{H-H} = 4.1 Hz, H_{14}), 4.29 (t, 2H, J_{H-H} = 3.7 Hz, H_{13}), 2.52 (s, 6H, $H_{3'}$, $H_{5'}$), 2.30 (q, 4H, J_{H-H} = 7.3 Hz, $H_{2'}$, $H_{6'}$), 1.98 (s, 3H, H_{17}), 1.33 (s, 6H, $H_{1'}$, $H_{7'}$), 0.98 (t, 6H, J_{H-H} = 7.3 Hz, $H_{2''}$, $H_{6''}$) ppm. ^{13}C NMR (100 MHz, $CDCl_3$): δ = 167.5 (C_{15}), 159.1 (C_{12}), 153.7, 140.2, 138.5, 136.1, 132.8, 131.3, 129.7 (C_{10}), 128.6, 126.3 (C_{18}), 115.3 (C_{11}), 66.1 (C_{13}), 63.1 (C_{14}), 18.5 (C_{17}), 17.2 ($C_{2'}$, $C_{6'}$), 14.8 ($C_{2''}$, $C_{6''}$), 12.6 ($C_{3'}$, $C_{5'}$), 12.0 ($C_{1'}$, $C_{7'}$) ppm. ^{19}F NMR (376 MHz, $CDCl_3$): δ = −145.7 (q, J_{F-B} = 32.3 Hz) ppm. ^{11}B NMR (128 MHz, $CDCl_3$): δ = −0.17 (t, J_{B-F} = 32.0 Hz) ppm. HRMS (ESI) m/z [M + Na]$^+$ calculated for $C_{29}H_{35}N_2O_3F_2BNa$, 531.2607; found, 531.2604 (100%). Mp =169 °C.

Synthesis of Monomer πEtA 4: 2,6-Diethyl-4,4-difluoro-8-(4-(2-acryloyloxy) ethoxy)phenyl)-1,3,5,7-tetramethyl-4-bora-3*a*,4*a*-diaza-*s*-indacene. The reaction was carried out using the same protocol as for πEtMA **3** using acryloyl chloride for the esterification. So, 43 mg of a pink powder were obtained from 88 mg of BODIPY πEtOH **7** (yield: 44%).

^{1}H NMR (400 MHz, $CDCl_3$): δ = 7.18 (d, 2H, J_{H-H} = 8.7 Hz, H_{10}), 7.02 (d, 2H, J_{H-H} = 9.1 Hz, H_{11}), 6.50 (d, 1H, J_{H-H} = 17.4 Hz, H_{17}), 6.21 (dd, 1H, J_{H-H} = 17.2, J_{H-H} = 10.3 Hz, H_{16}), 5.90 (d, 1H, J_{H-H} = 10.5 Hz, H_{17}), 2.53 (s, 6H, $H_{3'}$, $H_{5'}$), 2,30 (q, 4H, J_{H-H} = 7.6 Hz, $H_{2'}$, $H_{6'}$), 1.33 (s, 6H, $H_{1'}$, $H_{7'}$), 0.98 (t, 6H, J_{H-H} = 7.6 Hz, $H_{2''}$, $H_{6''}$) ppm. ^{13}C NMR (100 MHz, $CDCl_3$): δ = 166.3 (C_{15}), 159.0 (C_{12}), 153.7, 138.5, 132.8, 131.7, 131.3, 129.7 (C_{10}), 128.6, 128.2, 115.3 (C_{11}), 66.1 (C_{13}), 63.0 (C_{14}), 17.2 ($C_{2'}$, $C_{6'}$), 14.8 ($C_{2''}$, $C_{6''}$), 12.6 ($C_{3'}$, $C_{5'}$), 12.0 ($C_{1'}$, $C_{7'}$) ppm. ^{19}F NMR (376 MHz, $CDCl_3$): δ = −145.7 (q, J_{F-B} = 32.3 Hz) ppm. ^{11}B NMR (128 MHz, $CDCl_3$): δ = −0.15 (t, J_{B-F} = 33.2 Hz) ppm. HRMS (ESI) m/z [M + Na]$^+$ calculated for $C_{28}H_{33}N_2O_3F_2BNa$: 517.2445, found: 517.2447 (100%). mp =172 °C.

Synthesis of BODIPY πS 5: 2,6-Diethyl-4,4-difluoro-8-(4-vinylphenyl)-1,3,5,7-tetramethyl-4-bora-3*a*,4*a*-diaza-*s*-indacene. First, the 4-vinylbenzoyl chloride was synthesized in four steps following literature procedures. 4-Bromomethylbenzoic acid was obtained starting from the 4-methylbenzoic acid (7.90 g, yield: quantitative; ^{1}H NMR (400 MHz, $CDCl_3$): δ = 10.62 (bs, 1H, CO*OH*), 8.08 (d, 2H, J_{H-H} = 8.2 Hz, H_{Ar}), 7.49 (d, 2H, J_{H-H} = 8.2 Hz, H_{Ar}), 4.51 (s, 2H, *CH*$_2$-Br) ppm).[25] (4-Carboxybenzyl)-triphenylphosphonium bromide was obtained starting from 4-bromomethylbenzoic acid (6.49 g, yield: 45%; ^{1}H NMR (400 MHz, DMSO-d_6): δ = 12.88 (s, 1H, CO*OH*), 7.71−8.01 (m, 17H, H_{Ar}), 7.08

dx.doi.org/10.1021/ma400590q | *Macromolecules* XXXX, XXX, XXX−XXX

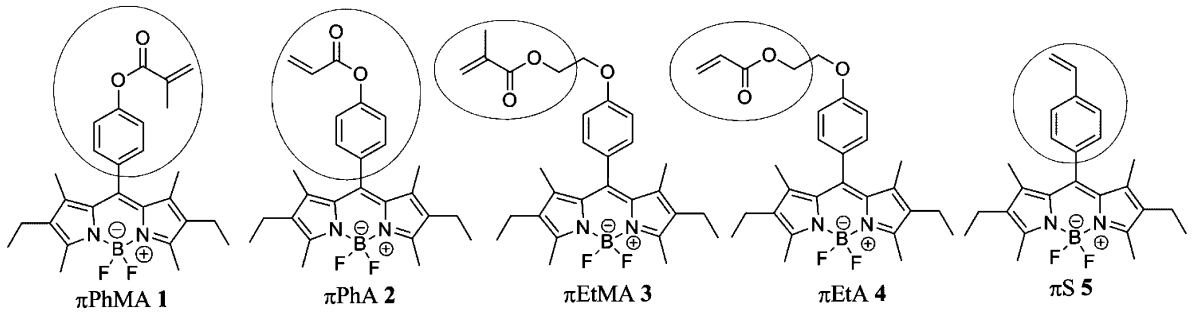

Figure 1. Molecular structure of the BODIPY monomers possessing different polymerizable functions.

(m, 2H, H_{Ar}), 5.25 (d, 2H, J_{H-P} = 12.01 Hz, CH_2−P) ppm).[26] 4-Vinylbenzoic acid was obtained starting from (4-carboxybenzyl)-triphenylphosphonium (2.14 g, 79%; ^{1}H NMR (400 MHz, $CDCl_3$): δ = 10.60 (bs, 1H, COOH), 8.07 (d, 2H, J_{H-H} = 8.2 Hz, H_{Ar}), 7.50 (d, 2H, J_{H-H} = 8.2 Hz, H_{Ar}), 6.77 (dd, 1H, J_{H-H} = 10.9, 17.5 Hz, CH═CH_2), 5.90 (d, 1H, J_{H-H} = 17.4 Hz, CH═CH_2), 5.42 (d, 1H, J_{H-H} = 11.0 Hz, CH═CH_2) ppm). To obtain the 4-vinylbenzoyl chloride, 4-vinylbenzoic acid (3.38 mmol, 0.5 g) was dissolved in 12 mL of chloroform. Then, thionyl chloride (10 equiv., 33.8 mmol, 4.02 g) was quickly added followed by one drop of DMF. The solution was heated under reflux for 5h. The mixture was purified by a short chromatography on silica gel (DCM). A yellow oil was obtained (yield: quantitative).

^{1}H NMR (400 MHz, $CDCl_3$): δ = 8.08 (d, 2H, J_{H-H} = 8.7 Hz, H_{10}), 7.52 (d, 2H, J_{H-H} = 8.7 Hz, H_{11}), 6.77 (dd, 1H, J_{H-H} = 11.0, 17.4 Hz, H_{13}), 5.95 (d, 1H, J_{H-H} = 17.4 Hz, H_{14}), 5.49 (d, 1H, J_{H-H} = 11.0 Hz, $H_{14'}$) ppm. ^{13}C NMR (100 MHz, $CDCl_3$): δ = 168.0 (C_8), 144.5 (C_{12}), 135.5 (C_{13}), 132.0 (C_9), 131.9 (C_{10}), 126.7 (C_{11}), 118.6 (C_{14}) ppm.

The 4-vinylbenzoyl chloride (2.0 mmol, 332 mg) was dissolved in 50 mL of dry dichloromethane and the solution placed in a round-bottom flask under argon. Kryptopyrrole (2.1 equiv., 4.2 mmol, 570 μL) was then added and the mixture heated under reflux for 2 h. Once the temperature decreased to room temperature, DIPEA (8 equiv., 16.0 mmol, 2.07 g) was added and 15 min later boron trifluoride diethyl etherate (11 equiv., 22 mmol, 3.12 g). The solvent was evaporated under vacuum and the residue purified by chromatography on silica gel (DCM). 60 mg of a pink powder were obtained (yield: 7%).

^{1}H NMR (400 MHz, $CDCl_3$): δ = 7.53 (d, 2H, J_{H-H} = 7.8 Hz, H_{11}), 7.24 (d, 2H, J_{H-H} = 8.2 Hz, H_{10}), 6.79 (dd, 1H, J_{H-H} = 10.8, 17.4 Hz, H_{13}), 5.86 (d, 1H, J_{H-H} = 17.4 Hz, H_{14}), 5.35 (d, 1H J_{H-H} = 11.0, $H_{14'}$), 2.53 (s, 6H, H3′, $H_{5'}$), 2.30 (q, 4H, J_{H-H} = 7.56, $H_{2'}$, $H_{6'}$), 1.32 (s, 6H, $H_{1'}$, $H_{7'}$), 0.98 (t, 6H, J_{H-H} = 7.6, $H_{2''}$, $H_{6''}$) ppm. ^{13}C NMR (100 MHz, $CDCl_3$): δ = 153.8, 140.1, 138.5, 138.1, 136.4 (C_{13}), 135.4, 132.9, 130.9, 128.7 (C_{10}), 126.9 (C_{11}), 114.9 (C_{14}), 17.2 ($C_{2'}$, $C_{6'}$), 14.8 ($C_{2''}$, $C_{6''}$), 12.6 ($C_{3'}$, $C_{5'}$), 12.0 ($C_{1'}$, $C_{7'}$) ppm. ^{19}F NMR (376 MHz, $CDCl_3$): δ = −145.7 (q, J_{F-B} = 32.9 Hz) ppm. ^{11}B NMR (128 MHz, $CDCl_3$): δ = −0.15 (t, J_{B-F} = 33.2 Hz) ppm. HRMS (ESI) m/z $[M + Na]^+$ calculated for $C_{25}H_{29}BF_2N_2Na$, 429.2284; found, 429.2289 (100%). Mp = 250 °C.

Synthesis of Fluorescent Nanoparticles by RAFT Miniemulsion Polymerization. The RAFT copolymerization of styrene and BODIPY monomers (initial feed 2 mol %) in the presence of PEO-*b*-PAA-C_{12} macro-RAFT agent in a one-pot phase inversion process was performed as described elsewhere.[14]

First, the PEO-*b*-PAA-C_{12} macro-RAFT agent was synthesized according to reference14 in 1,4-dioxane at 80 °C under argon atmosphere: In a typical experiment, the PEO-based trithiocarbonate macro-RAFT agent,[14] PEO-C_{12}, (0.5 mmol, 1.21 g, M_n = 2420 g/mol), acrylic acid (10 mmol, 720 mg), and DMF (as an internal reference for the ^{1}H NMR determination of the monomer consumption in deuterated chloroform) (2 mmol, 146 mg) were dissolved in 4.9 mL of 1,4-dioxane at room temperature. Then, 0.1 mL of a 0.33 M solution of ACPA in 1,4-dioxane was added. The mixture is purged with nitrogen for 30 min in an ice bath, then placed in an oil bath thermostated at 80 °C to initiate the polymerization. After 90 min, the reaction was stopped by immersion of the flask in iced water. The monomer conversion was determined by ^{1}H NMR in $CDCl_3$. The copolymer was dried under reduced pressure in order to remove the residual acrylic acid monomer. PEO_{45}-*b*-PAA_{18}-C_{12} macro-RAFT agent ($M_{n,th}$ = 3.7, $M_{n,SEC}^{PS}$ = 4.6, M_w/M_n = 1.14) composed of a PEO block of M_n = 2.0 kg/mol and a PAA block of M_n = 1.7 kg/mol was obtained.

Then, in a typical experiment of the nanoparticles synthesis, 140 mg of PEO-*b*-PAA-C_{12} macro-RAFT (4.0×10^{-5} mol, M_n = 3.7 kg/mol) was dissolved in a mixture of 650 mg of styrene (6.3×10^{-3} mol), 2.2 mg of AIBN (1.3×10^{-5} mol) and 58 mg of monomer πPhA **2** (1.3×10^{-4} mol), in a septum-sealed flask. The mixture was purged with argon for 30 min in an ice bath, and then placed in an oil bath thermostatically controlled at 80 °C to initiate polymerization. After 70 min, the reaction was stopped by immersion of the flask in iced water. The conversion of the monomers (styrene and BODIPY derivative) was determined by gravimetry and SEC, respectively (for details see below). To the cold organic mixture, 5 mL of basic water (pH = 12.5) was added. An ultrasonic horn (Bandelin electronics, Sonoplus HD 2200) is then placed in the biphasic mixture cooled down in an ice bath and powered at 130 W for 10 min.

After the miniemulsion formation, the pH decreased to 11. The miniemulsion is purged with argon for 30 min in an ice bath, and then placed in an oil bath thermostatically controlled at 80 °C to reinitiate the polymerization. Sampling is performed at regular time intervals and monomer conversions are determined by gravimetric analysis for styrene corrected from the styrene loss by evaporation during the sonication process (25 wt % calculated by comparison of ^{1}H NMR spectra in $CDCl_3$ and gravimetric analysis (see Figure SI-9, Supporting Information); considering this the molar percentage of BODIPY monomer was therefore corrected to 2.6 ± 0.1 mol %[30]) and by SEC using the UV−visible detection for BODIPY monomers (Table 2).

RESULTS AND DISCUSSION

Synthesis and Characterization of BODIPY Monomers. Four novel fluorescent BODIPY derivatives possessing different polymerizable functions have been synthesized (Figure 1): BODIPY phenyl acrylate (πPhA, **2**), BODIPY ethyl methacrylate (πEtMA, **3**), BODIPY ethyl acrylate (πEtA, **4**) and BODIPY styrene (πS, **5**) in order to compare them with the previously reported phenyl methacrylate BODIPY (πPhMA, **1**).[14]

Monomers πPhMA **1** and πPhA **2** were synthesized starting from a BODIPY bearing a phenol function (**6**) on the *meso* position (Scheme SI-1, Supporting Information). The latter was synthesized via a conventional one-pot three steps approach by reacting 2 equiv of kryptopyrrole with one equivalent of 4-hydroxybenzaldehyde (yield: 80%).[14] To obtain the monomers, a classical esterification of the BODIPY phenol **6** was performed in presence of either methacryloyl chloride to

dx.doi.org/10.1021/ma400590q | Macromolecules XXXX, XXX, XXX−XXX

obtain the monomer πPhMA **1** (yield: 78%), or acryloyl chloride to obtain the monomer πPhA**2** (yield: 50%).

Syntheses of monomers πEtMA **3** and πEtA **4** were first attempted from the same BODIPY phenol **6**. However, all trials to effect a Williamson reaction on the phenol with 2-bromoethanol or 2-bromoethyl methacrylate failed and led to the degradation of compound **6**. An alternative reaction scheme was therefore established (Scheme SI-2, Supporting Information), in which 4-(2-hydroxyethoxy)benzaldehyde was synthesized first by a Williamson reaction of 4-hydroxybenzaldehyde with 2-bromoethanol. The BODIPY framework **7** was then formed from this new aldehyde and kryptopyrrole (yield: 72%). Then, monomers πEtMA **3** and πEtA **4** were successfully obtained by esterification of the alcohol with methacryloyl chloride (yield: 50%) and acryloyl chloride (yield: 44%), respectively.

At last, monomer πS **5** was synthesized via another conventional route for BODIPY synthesis (Scheme SI-3),[27] using 4-vinylbenzoyl chloride which was synthesized in four steps and 21% overall yield starting from 4-methylbenzoic acid using a Wittig reaction as the key step. Monomer πS **5** was then obtained by reacting 4-vinylbenzoyl chloride with kryptopyrrole in low (7%) but not optimized yield.

Absorption and fluorescence spectra of the BODIPY-based monomers recorded in toluene are shown in Figure 2 and their

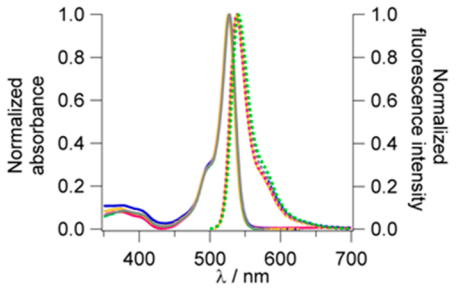

Figure 2. Absorption (full lines) and fluorescence spectra (dotted lines, λ_{exc} = 495 nm) of the BODIPY monomer derivatives recorded in toluene. Monomers πPhMA **1** (green line), πPhA **2** (gray line), πEtMA **3** (yellow line), πEtA **4** (pink line), and πS **5** (blue line).

spectroscopic properties are given in Table 1. All monomers had a maximum of absorption around 527 nm and a maximum of fluorescence emission between 538 and 540 nm. They all showed a quantum yield (Φ_F) around 70%, a usual value for that kind of BODIPY.[28]

In addition, time-resolved fluorescence measurements were performed in toluene (Figure 3). Fluorescence decays could be fitted by a monoexponential function (Figures SI-3−SI-7, Supporting Information) and lifetimes were found to be between 4.1 and 4.9 ns. Monomer πS **5** had a lifetime shorter than the other monomeric derivatives but its radiative decay

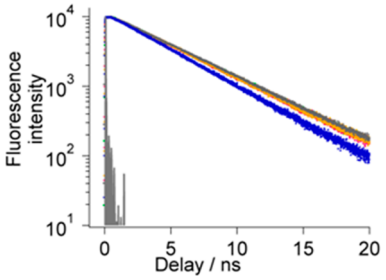

Figure 3. Fluorescence decays of the different BODIPY monomers in toluene. Monomers πPhMA **1** (green line), πPhA **2** (gray line), πEtMA **3** (yellow line), πEtA **4** (pink line) and πS **5** (blue line). The instrument response function (IRF) is presented in light gray (λ_{exc} = 495 nm, λ_F = 543 nm).

rate was of the same order (1.73×10^8 s^{-1} vs. ~1.5×10^8 s^{-1} for the others). Since all monomers exhibit the same fluorescent framework (same substituents on the pyrroles and a phenyl group on the *meso* position), it is not surprising that they display similar spectroscopic properties. This will allow for an easier comparison of the spectroscopic properties of the nanoparticles.

Synthesis of the Fluorescent Nanoparticles. We previously reported[14] the synthesis of fluorescent polymer nanoparticles via controlled radical RAFT polymerization in miniemulsion, using a surfactant-free one-pot phase inversion process (Scheme 1). The selected synthetic approach relied on the polymerization-induced self-assembly (PISA[29]) principle where amphiphilic copolymers form during polymerization and assemble simultaneously into core−shell particles. In more details, a fluorescent BODIPY monomer (π) was copolymerized with styrene (S) in the presence of a poly(ethylene oxide)-*b*-poly(acrylic acid) macro-RAFT agent, PEO-*b*-PAA-C_{12}, first in bulk and—after phase inversion—in miniemulsion. PEO-*b*-PAA-*b*-P(S-*co*-π) triblock copolymers formed and self-assembled *in situ* during the miniemulsion step affording well-defined core−shell nanoparticles with a fluorescent core and a biocompatible and reactive shell (see cartoons in Figure 4, schematic representation of the NP, and Scheme SI-4, Supporting Information for the synthetic approach). In this former study (NP1 in Table 2), the core was made of styrene copolymerized with 2.6 mol %[30] of monomer πPhMA **1**, and the shell was a PEO-*b*-PAA diblock copolymer with a number-average molar mass, M_n, of PEO of 2 kg/mol and that of PAA was 1 kg/mol. The final particles had a hydrodynamic diameter about 65 nm (σ ~ 0.1) and an aggregation number (i.e., an average number of copolymer chains per particle) of 1750 (±250).[17]

Using the same synthetic strategy (Scheme 1, Scheme SI-4, Supporting Information), in this work four novel types of fluorescent nanoparticles (Table 2) were synthesized by

Table 1. Spectroscopic Properties of the BODIPY Monomer Derivatives Recorded in Toluene at 20 °C

monomer	λ_{abs}/nm	λ_F/nm	Φ_F	ε (×10^{-3}) L·mol^{-1}·cm^{-1}	τ^a/ns	k_r/10^{-8} s^{-1}	k_{nr}/10^{-7} s^{-1}	B^b (×10^{-3}) L·mol^{-1}·cm^{-1}
πPhMA **1**	528	540	0.69	73	4.9	1.41	6.33	50.4
πPhA **2**	528	540	0.74	79	4.8	1.54	5.42	58.5
πEtMA **3**	527	538	0.75	70	4.8	1.56	5.21	52.5
πEtA **4**	527	538	0.71	74	4.7	1.49	6.38	52.5
πS **5**	527	539	0.71	68	4.1	1.73	7.07	48.3

[a]Decay fitted with a monoexponential function (λ_{exc} = 495 nm, λ_F = 543 nm). [b]Molecular brightness, $B = \varepsilon \times \Phi_F$.

dx.doi.org/10.1021/ma400590q | *Macromolecules* XXXX, XXX, XXX−XXX

Scheme 1. Synthetic Pathway for the Synthesis of the Fluorescent Nanoparticles

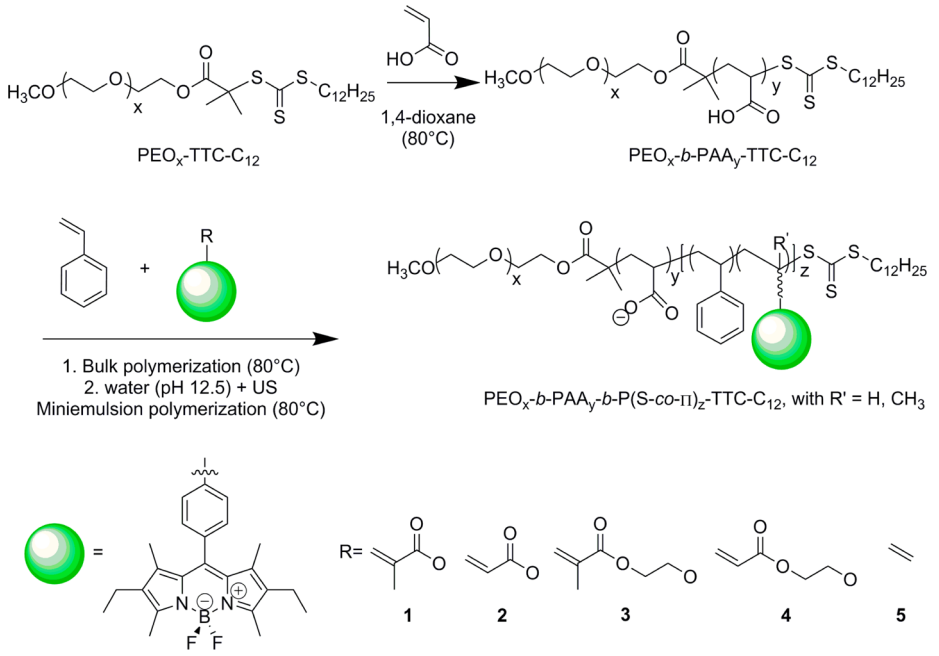

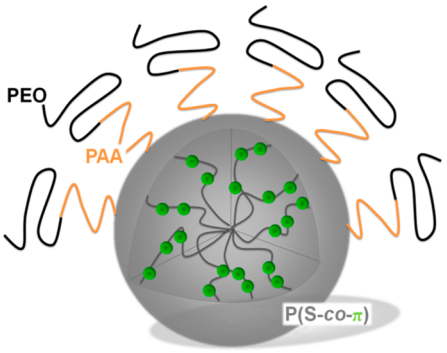

Figure 4. Schematic representation of the fluorescent core−shell nanoparticles.

copolymerizing 2.6 mol %[30] of the different BODIPY monomers **2**−**5** with styrene. The target degree of polymerization, DP_n, was about 120 in all cases (initial monomer to macro-RAFT agent molar ratio of 160, which leads to 120 considering the 25% of styrene evaporation).[30] The final particle size distributions were all monomodal with an average hydrodynamic diameter D_z ranging from 60 to 90 nm. Size exclusion chromatography analyses on unpurified crude samples taken from the reaction medium in regular time intervals allowed not only following the consumption of the PEO-*b*-PAA-C_{12} macro-RAFT agent during the polymerization with the formation of well-defined growing PEO-*b*-PAA-*b*-P(S-*co*-*π*) triblock copolymers (Figure 5 left, RI response), but also confirmed the successful incorporation of the fluorescent comonomer in the triblock copolymer. Indeed, using SEC with an in-line UV−vis. detection set at the maximum absorption wavelength of the monomers (λ_{abs} = 528 nm) made possible the separation of the fluorescent monomer, eluted at around 18 mL, from the fluorescent triblock copolymer eluted between 13.5 and 16 mL (Figure 5, right, UV−vis response at λ = 528 nm). The absorption of the formed triblock copolymers at 528 nm undoubtedly confirms the covalent incorporation of the fluorescent monomer in the polymer chain. In addition, this detection mode also allows following the fluorescent monomer consumption and the calculation of the fluorescent monomer's individual conversion by comparison of both the monomer's and the polymer's signal areas.

Table 2. Experimental Results of the Different Fluorescent Nanoparticles (NP) Having Different BODIPY Monomers in their Cores

NP	BODIPY monomer	n_π[a]	convn$_S$[b]	convn$_\pi$[c]	$M_{n,th}$[d]/kg/mol	$M_{n,SEC}$[e]/kg/mol	M_w/M_n[e]	D_z (σ)[f]/nm
NP1	*π*PhMA **1**	3.0	0.99	0.98	16.4	21.0	1.25	65 (0.08)
NP2	*π*PhA **2**	2.9	0.95	0.95	16.1	16.1	1.50	60 (0.13)
NP3	*π*EtMA **3**	3.2	1.00	0.98	17.3	19.0	1.40	85 (0.21)
NP4	*π*EtA **4**	3.2	0.9	0.95	15.3	16.8	1.26	90 (0.05)
NP5	*π*S **5**	3.1	0.94	0.92	12.6	13.9	1.46	75 (0.20)

[a]Average number of BODIPY monomers per polymer chain (with a $DP_{n,total}$ about 120; Figure SI-8, Supporting Information). [b]Styrene conversion determined by gravimetry. [c]BODIPY conversion determined by SEC by comparison of the calculated area of the polymer and monomer peaks from SEC equipped with a UV−vis detector.[14] [d]Theoretical number-average molar mass ($M_{n,th}$) ($M_{n,th} = M_{n\ CTA} + 1/n_{CTA} \times (\text{convn}_S \times m_S$[30] $+ \text{convn}_\pi \times m_\pi$), where CTA stands for chain transfer agent, convn$_S$[30] and convn$_\pi$ the individual conversion of styrene and BODIPY monomer and m the mass of monomer used in the synthesis). [e]Number-average molar mass ($M_{n,SEC}$) and polydispersity index (M_w/M_n) determined by SEC using a polystyrene calibration. [f]*z*-average diameter (D_z) and dispersity factor (σ) determined by DLS.

dx.doi.org/10.1021/ma400590q | *Macromolecules* XXXX, XXX, XXX−XXX

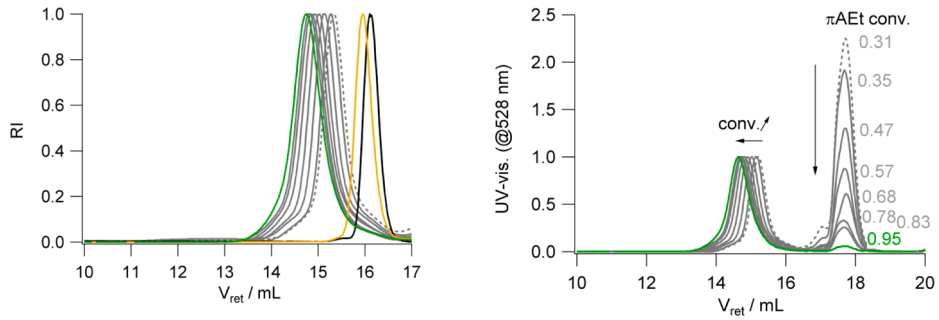

Figure 5. Monitoring of the synthesis of nanoparticles **4** (with πEtA) by size exclusion chromatography in THF. Left: RI detection. Right: UV−vis detection at the maximal absorption of the monomer πEtA **4** (λ = 528 nm). (macro-RAFT agents: black line, PEO-C_{12}; yellow line, PEO-*b*-PAA-C_{12}; PEO-*b*-PAA-*b*-P(S-*co*-π)-C_{12}: gray dots, end of bulk polymerization; gray lines, during miniemulsion polymerization; green line, end of miniemulsion polymerization.

Figure 6 shows the final SECs for the different NPs samples at the end of the polymerization, without purification (Table 2,

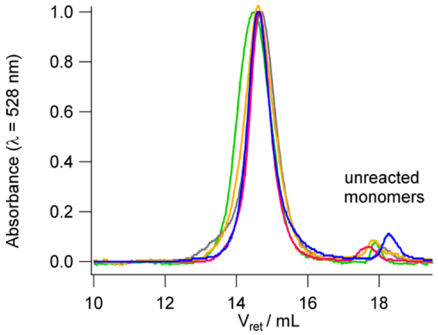

Figure 6. Size exclusion chromatograms (UV−vis. detection, λ = 528 nm) in THF for polymer chains of nanoparticles with different BODIPY monomers (πPhMA **1** (green line), πPhA **2** (gray line), πEtMA **3** (yellow line), πEtA **4** (pink line), and πS **5** (blue line)).

NP1 to NP5 made with the different fluorescent monomers). For all samples, the great majority of the fluorescent monomer molecules was incorporated into the polymer chains (V_{ret} ~ 15 mL) and only a negligible fraction was left over (V_{ret} ~ 18 mL). From the relative integration of the peaks it was calculated that the individual monomer conversion of all BODIPY monomers was high (conv. > 0.90), meaning that the new fluorescent monomers **2**−**5** can be copolymerized with styrene under the conditions established before for monomer **1**. For all fluorescent monomers the calculated ($M_{n,th}$) and experimental ($M_{n,SEC}$) number-average molar mass values were close, and M_w/M_n remained below 1.5, meaning that the polymerization was under RAFT control.

In order to determine the distribution of the BODIPY monomers along the polymer chains the individual conversions of both styrene and of the BODIPY monomers were monitored in the course of the nanoparticles synthesis. For each copolymerization system, the molar fraction of BODIPY incorporated into the copolymer could then be calculated with respect to the overall molar conversion (Figure 7).

The overall monomer molar conversion was then determined as follows:

$$\text{convn}_{\text{total}}\,(\text{mol}) = \text{convn}_S\frac{n_S}{n_{\text{total}}} + \text{convn}_\pi\frac{n_\pi}{n_{\text{total}}} \qquad (3)$$

Where convn_S and convn_π are the individual conversion of styrene (determined by gravimetry) and of the BODIPY

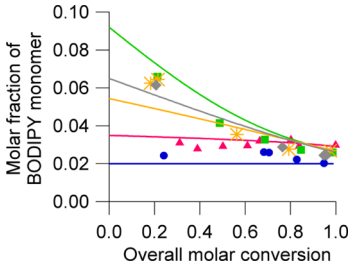

Figure 7. Evolution of the average molar fraction of BODIPY monomer in the copolymer with the overall molar monomer conversion (symbols, experimental values; lines, calculated with the reactivity ratios; initial molar fraction of BODIPY monomer = 2.6 mol %). Monomers πPhMA **1** (green ■ and line, r_S = 0.25, r_{PhMA} = 0.50[18]), πPhA **2** (gray ◆ and line, r_S = 0.38 determined by the Kelen-Tüdös method, r_{PhA} estimated at 0.50),[31] πEtMA **3** (yellow ∗ and line, r_S = 0.46, r_{EtMA} = 0.38[32]), πEtA **4** (pink ▲ and line, r_S = 0.8, r_{EtA} = 0.2[33]), πS **5** (blue ● and line, r_S = 1, r_S = 1).

monomer (determined from the areas of the signal of the polymer and the monomer in the size exclusion chromatogram using UV−vis. detection, Figure 5, right), and n_S, n_π, and n_{total} are respectively the mole number of styrene and BODIPY monomer and the total mole number of styrene and BODIPY used in the synthesis.

The symbols in Figure 7 are the experimentally determined average molar fraction of the different BODIPY monomers incorporated in the copolymers, plotted as a function of the overall molar monomer conversion. Two tendencies can mainly be observed: the BODIPY monomer is either quickly incorporated in the polymer chain (πPhMA **1**, πPhA **2** and πEtMA **3**) leading to a gradient of composition in the polymer chain, or the BODIPY monomer is homogeneously and quasi randomly distributed in the polymer backbone (πS **5** and πEtA **4**). Unlike the other monomers, for BODIPY monomers πEtA **4** and πS **5**, given the low amount of BODIPY monomer in the copolymer (~2.6 mol %), one may assume that the fluorescent monomer units are well separated by large polystyrene segments, which could have an impact on the fluorescence properties.

As mentioned above, in a controlled radical polymerization, all polymer chains possess approximately the same composition and their microstructure is determined by the reactivity ratios r_{M1} and r_{M2} in the terminal model. Reactivity ratios of simple monomers possessing the same polymerizable functions as the new fluorescent monomers have been extensively tabulated.[18] The fluorophore framework of the BODIPY monomers is not

dx.doi.org/10.1021/ma400590q | *Macromolecules* XXXX, XXX, XXX−XXX

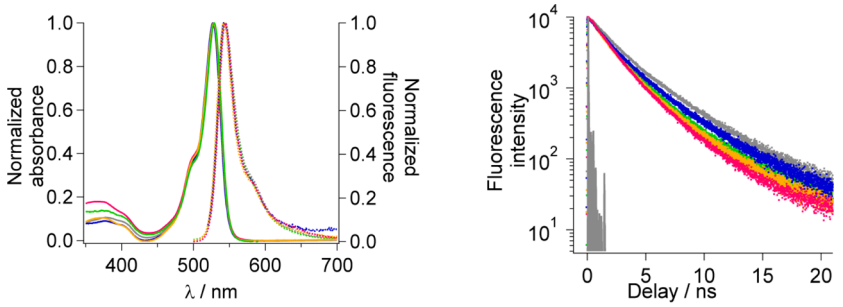

Figure 8. Spectra of nanoparticles with different BODIPY monomers (πPhMA (green line), πPhA (gray line), πEtMA (yellow line), πEtA (pink line), and πS (blue line) recorded in water. Left: absorption (full lines) and emission (dotted lines, λ_{exc} = 495 nm) spectra. Right: fluorescence decays (light gray line is the instrument response function, λ_{exc} = 495 nm, λ_F = 543 nm).

Table 3. Fluorescence Properties of Different Nanoparticles Recorded in Water

NP	monomer	n_π [a]	$\lambda_{abs\ max}$/nm	λ_F/nm	Φ_F [b]	$\langle\tau\rangle$ [c]/ns	B [d] ($\times 10^{-7}$)/L·cm^{-1}·mol^{-1}
NP1	πPhMA **1**	3.0	529	544	0.20 (±0.02)	2.8	7.7
NP2	πPhA **2**	2.9	529	544	0.35 (±0.03)	3.6	14.0
NP3	πEtMA **3**	3.2	528	542	0.28 (±0.02)	2.7	11.0
NP4	πEtA **4**	3.2	528	544	0.23 (±0.03)	2.6	9.5
NP5	πS **5**	3.1	527	542	0.34 (±0.02)	3.1	13.0

[a]Average number of BODIPY monomers per chain ($n_\pi = [\pi]_0/[RAFT]_0$). [b]Average fluorescence quantum yield calculated for two different nanoparticles synthesis and, in parentheses, deviation from the average. [c]Average fluorescence lifetime (λ_{exc} = 495 nm, λ_F = 543 nm) calculated as $\langle\tau\rangle \equiv \frac{\int_0^\infty tI(t)\,dt}{\int_0^\infty I(t)\,dt}$ (eq 1). [d]Nanoparticles brightness, calculated using eq 4 with ε taken at $\lambda_{abs\ max}$ (527 or 528 nm) and N_{agg} = 1750 (see Supporting Information for calculation).

conjugated to the polymerizable vinyl groups, and their reactivity should therefore not significantly differ from that of the corresponding simple monomer structures in their radical copolymerization with styrene (even if steric effects may arise[34]). The continuous lines in Figure 7 represent the average molar fractions calculated by the Skeist equation[35] knowing the initial molar fraction of the BODPY monomer and using the reactivity ratios tabulated for the corresponding model monomers, i.e., styrene (S) for πS **5**, phenyl methacrylate (PhMA) for πPhMA **1** etc.).[18,31−33] In all cases the plots matched well the experimental data points. It can thus be concluded that the tabulated reactivity ratios for model monomers are valid to estimate the microstructure in the fluorescent copolymer.

In the next part, the fluorescence properties of the different fluorescent nanoparticles are studied.

Spectroscopic Characterization of the Fluorescent Nanoparticles. Absorption and fluorescence emission spectra of the nanoparticles are reported in Figure 8. It appears that the nanoparticles in water have the same absorption and emission spectra as their monomers recorded in toluene. In order to evaluate the formation of poorly fluorescent aggregates, the quantum yield and average fluorescence lifetimes (see eq 1) of the nanoparticles were compared (Table 3). Particles with the lowest quantum yield and lifetimes were particles with a core made of the monomers πPhMA **1** and πEtA **4** (Φ_F < 0.25 and $\langle\tau\rangle$ < 3 ns). In contrast, particles with the highest quantum yield were particles with a core made of πS **5** and πPhA **2** (Φ_F > 0.30 and $\langle\tau\rangle$ > 3 ns). Particles with a core of πEtMA **3** showed intermediate properties.

How can the differences in the fluorescence properties be explained? One possible explanation which might be considered relies on the differences of the fluorescent monomer distribution in the copolymer chain constituting the fluorescent nanoparticles. Gradient compositions lead to an increased proximity of the fluorescent monomer which might lead to quenching caused by poorly fluorescent intrachain aggregates. In addition, a favorable incorporation of the fluorescent monomer from the beginning or at the end of the polymerization might lead to particles where the fluorophores are concentrated either in the inner core or close to the hydrophilic shell.

According to our kinetic study, monomer πS **5** is homogeneously spread along the polymer chain and the resulting particles possess high quantum yields and brightness. On the other hand, πPhMA **1** is heterogeneously spread along the polymer chain and leads to nanoparticles with much poorer fluorescence properties. For these two examples, it seems that a correlation between the microstructure of the polymer chains and fluorescence properties exists.

However, regarding monomer **4** (πEtA), which possesses also a quasi-random distribution of the fluorophores in the polymer chain, a poor quantum yield and the lowest average fluorescence lifetime of the series were determined. A quasi-random distribution of the BODIPY monomer in the polymer chain constituting the nanoparticle (case of monomer πS **5** and πEtA **4**) does not necessarily lead to the most fluorescent particles, and vice versa, BODIPY monomers which are not evenly spread along the polymer backbone (for instance πPhA) do not unavoidably lead to the less fluorescent particles. It must therefore be concluded that the fluorescence properties (quantum yield and lifetime) do not exclusively depend on the distribution of the fluorescent monomer in the polymer chain, but that other parameters must also be considered, such as the organization of the polymer chains in the nanoparticle during the assembly step occurring during synthesis, the formation of interchain aggregates etc. Indeed, because of the confined space of the polymeric chains in the nanoparticles,

dx.doi.org/10.1021/ma400590q | Macromolecules XXXX, XXX, XXX−XXX

aggregates of fluorescent monomers between different polymer chains may form. Their formation might depend on the BODIPY monomers' orientation in the polymer chain or on differences in solubility of the monomers in the organic phase (made of styrene and PEO-*b*-PAA-C_{12} macro-RAFT agent), possibly leading to a local phase separation during the polymerization process.

The nanoparticle brightness (B), which is a function of the quantum yield and in practice one of the most important features for biological imaging, was also evaluated from eq 4:

$$B = (\varepsilon_\pi \times N_\pi) \times \phi_F \quad (4)$$

where ε_π is the molar coefficient extinction of the BODIPY monomer at the excitation wavelength, N_π the number of BODIPY per particle (equation SI-3, Supporting Information) and Φ_F the quantum yield of the fluorescent nanoparticle.

For all systems, brightness values higher than 7×10^7 $cm^{-1}{\cdot}mol^{-1}{\cdot}L$ were obtained (Table 3). They were all in the same order of magnitude, but NP containing monomer πPhA **2** and πS **5**, possessing the best quantum yields, were the brightest ones (respectively 14×10^7 and 13×10^7 $cm^{-1}{\cdot}mol^{-1}{\cdot}L$). For comparison, the NP prepared in our former study with monomer πPhMA **1** had a brightness of 7.7×10^7 $cm^{-1}{\cdot}mol^{-1}{\cdot}L$. It is thus possible to increase the brightness of the fluorescent nanoparticles by a factor of 1.8, only by changing the nature of the fluorescent monomer in the core.

Quantum dots are famous for their extremely high brightness making them ideal candidates for biological imaging. Generally, quantum dots with a core made of CdSe, CdS, or CdTe emitting between 370 and 750 nm have a brightness between 6×10^4 and 6×10^5 $cm^{-1}{\cdot}mol^{-1}{\cdot}L$.[36] The fluorescent nanoparticles NP2 with a core of monomer πPhA **2** are thus 200 to 2000 times brighter than those quantum dots. Compared to most of other systems based on fluorescent organic polymeric nanoparticles, NP2 are on average 40 to 300 times brighter. For instance, Sun et al. have synthesized nanoparticles (diameter: 20−25 nm) made of PEO_{113}-*b*-$PVBA_{46}$-C_{12} (PVBA: poly(4-vinylbenzaldehyde)) functionalized with a fluorescein dye. The best nanoparticles have a brightness of 5.1×10^5 $cm^{-1}.mol^{-1}.L$.[3b] Méallet-Renault et al. have loaded 16 nm diameter polystyrene nanoparticles with a BODIPY derivative dye by the solvent displacement method.[37] With approximately 76 BODIPY molecules per particle and a quantum yield of 0.77, the nanoparticles had a brightness of 3.4×10^6 $cm^{-1}.mol^{-1}.L$.

In conclusion, it is possible to modulate the fluorescence efficiency simply by changing the nature of the fluorescent BODIPY monomer, and thus its distribution within the polymer backbone. Nevertheless, it is difficult to predict the formation of BODIPY aggregates in the fluorescent polymer nanoparticles, by considering exclusively aggregates along the polymer backbone (intrachain aggregates) and disregarding aggregate formation between fluorescent polymer chains (interchain aggregates).

Finally, it should be emphasized that the BODIPY monomer with a phenyl acrylate polymerizable function (πPhA **2**) is the best candidate for future NP design since it is the easiest to synthesize leading to ultrabright NP.

CONCLUSIONS

Five BODIPY derivatives with different polymerizable functions were successfully synthesized and their fluorescence properties were studied in toluene. All fluorophores could be successfully copolymerized at 2.6 mol % with styrene in a controlled manner via our formerly established one-pot RAFT miniemulsion polymerization process in the absence of surfactant. This route to form fluorescent polymeric core shell nanoparticles is thus a robust method and should be applicable to a large variety of fluorescent molecules. We have further demonstrated that the microstructure of the resulting copolymers is governed by the nature of the polymerizable function on the BODIPY, and that the fluorescent monomer distribution can be predicted by using reactivity ratios tabulated for the corresponding model monomers.

The fluorescence features of the nanoparticles were studied by stationary and time-resolved spectroscopy. Surprisingly, the most fluorescent nanoparticles (in terms of lifetime, quantum yield and thus brightness) were not necessarily obtained with the quasi-random polymer structure. It must thus be concluded that not only intrachain aggregates of BODIPY monomers must be considered, but that fluorophores' interchain aggregates and maybe the solubility of the different fluorescent monomers in the nanoparticle core matrix are of crucial importance for the outcome of the fluorescence properties. Nevertheless, simply by changing the nature of the polymerizable function on the BODIPY (to a phenyl acrylate or styrene function), the brightness of the nanoparticles could be improved by a factor of 2 compared to the formerly studied BODIPY monomer bearing a phenyl methacrylate function. Those ultrabright nanoparticles were found to be 200 to 2000 times brighter than usual quantum dots and 40−300 times brighter than other polymeric nanoparticles reported in the literature.

ASSOCIATED CONTENT

Supporting Information

Synthetic schemes for BODIPY monomers **1**−**5** and the fluorescent nanoparticles; numbering of protons and carbons of BODIPY monomers **2**−**5**; determination of the reactivity ratio r_s for the copolymerization of styrene with πPhA **2** by the Kelen-Tüdös method; fluorescence decays, fit, instrument response function (IRF), and residuals for all monomers; ^{1}H NMR spectra of dried and crude **NP4**; and determination of the aggregation number and the number of BOPIDY units per NP. This material is available free of charge via the Internet at http://pubs.acs.org.

AUTHOR INFORMATION

Corresponding Author

*E-mail: jutta.rieger@upmc.fr (J.R.); gilles.clavier@ppsm.ens-cachan.fr (G.C.).

Notes

The authors declare no competing financial interest.

ACKNOWLEDGMENTS

The authors thank Gaëlle Pembouong (LCP) for technical support on SEC analyses and Arnaud Brosseau (PPSM) for technical support on fluorescence spectroscopy measurements. B. C. acknowledges the Institut Universitaire de France for her nomination as a senior member.

REFERENCES

(1) (a) Rosi, N. L.; Mirkin, C. A. *Chem. Rev.* **2005**, *105*, 1547−1562. (b) Louie, A. *Chem. Rev.* **2010**, *110*, 3146−3195. (c) Hu, J.; Liu, S. *Macromolecules* **2010**, *43*, 8315−8330.

(2) (a) Qin, W.; Rohand, T.; Dehaen, W.; Clifford, J. N.; Driesen, K.; Beljonne, D.; Van Averbeke, B.; Van der Auweraer, M.; Boens, N. *J Phys. Chem. A* **2007**, *111*, 8588−8597. (b) Sauer, R.; Turshatov, A.; Baluschev, S.; Landfester, K. *Macromolecules* **2012**, *45*, 3787−3796.

(3) (a) Palma, A.; Tasior, M.; Frimannsson, D. O.; Vu, T. T.; Méallet-Renault, R.; O'Shea, D. F. *Org. Lett.* **2009**, *11*, 3638−3641. (b) Sun, G.; Berezin, M. Y.; Fan, J.; Lee, H.; Ma, J.; Zhang, K.; Wooley, K. L.; Achilefu, S. *Nanoscale* **2010**, *2*, 548−558.

(4) Hu, J.; Zhang, X.; Wang, D.; Hu, X.; Liu, T.; Zhang, G.; Liu, S. *J. Mater. Chem.* **2011**, *21*, 19030−19038.

(5) Sun, H.; Scharff-Poulsen, A. M.; Gu, H.; Almdal, K. *Chem. Mater.* **2006**, *18*, 3381−3384.

(6) Montalti, M.; Prodi, L.; Zaccheroni, N.; Zattoni, A.; Reschiglian, P.; Falini, G. *Langmuir* **2004**, *20*, 2989−2991.

(7) Matyjaszewski, K. *Macromolecules* **2012**, *45*, 4015−4039.

(8) Moad, G.; Rizzardo, E.; Thang, S. H. *Polymer* **2008**, *49*, 1079−1131.

(9) C. Barner-Kowollik (ed.), *Handbook of RAFT Polymerization*; Wiley-VCH: Weinheim, Germmany, 2008.

(10) Nagai, A.; Yoshii, R.; Otsuka, T.; Kokado, K.; Chujo, Y. *Langmuir* **2010**, *26*, 15644−15649.

(11) (a) You, J.; Yoon, J. A.; Kim, J.; Huang, C.-F.; Matyjaszewski, K.; Kim, E. *Chem. Mater.* **2010**, *22*, 4426−4434. (b) Li, C.; Zhang, Y.; Hu, J.; Cheng, J.; Liu, S. *Angew. Chem., Int. Ed.* **2010**, *49*, 5120−5124.

(12) Matyaszewski, K., Gnanou, Y., Leibler, L., Eds. *Macromolecular Engineering*; Wiley-VCH: Weinheim, Germany, 2007.

(13) Tronc, F.; Li, M.; Lu, J.; Winnik, M. A.; Kaul, B. L.; Graciet, J.-C. *J. Polym. Sci., Part A: Polym. Chem.* **2003**, *41*, 766−778.

(14) Grazon, C.; Rieger, J.; Méallet-Renault, R.; Clavier, G.; Charleux, B. *Macromol. Rapid Commun.* **2011**, *32*, 699−705.

(15) Loudet, A.; Burgess, K. *Chem. Rev.* **2007**, *107*, 4891−4932.

(16) Grazon, C.; Rieger, J.; Charleux, B.; Clavier, G.; Méallet-Renault, R. To be published.

(17) Grazon, C. Ph.D. Dissertation. ENS Cachan: Cachan, France, 2012.

(18) Brandrup, J.; Immergut, E. H.; Grulke, E. A.; Abe, A.; Bloch, D. R., *Polymer Handbook*; John Wiley & Sons, Inc: New York, 1999; pp II-181−II-308.

(19) (a) Yan, Y.; Lu, N.; Cui, J.; Zhang, J. *J. Appl. Polym. Sci.* **2012**, *125*, 2867−2873. (b) Morishima, Y.; Sang Lim, H.; Nozakura, S.-i. *Macromolecules* **1989**, *22*, 1148−1154.

(20) Couvreur, L.; Lefay, C.; Belleney, J.; Charleux, B.; Guerret, O.; Magnet, S. *Macromolecules* **2003**, *36*, 8260−8267.

(21) Kubin, R. F.; Fletcher, A. N. *J. Lumin.* **1982**, *27*, 455−462.

(22) Valeur, B. *Molecular Fluorescence: Principles and Applications*; Wiley-VCH: Weinheim, Germmany, 2002.

(23) Dumas-Verdes, C.; Miomandre, F.; Lépicier, E.; Galangau, O.; Truc Vu, T.; Clavier, G.; Méallet-Renault, R.; Audebert, P. *Eur. J. Org. Chem.* **2010**, 2525−2535.

(24) Roncucci, G.; Dei, D.; Giuntini, F.; Chiti, G.; Nistri, D.; Fantetti, L.; Paschetta, V.; Cocchi, A. WO/2004/035590 patent, 2004.

(25) Kikuchi, D.; Sakaguchi, S.; Ishii, Y. *J. Org. Chem.* **1998**, *63*, 6023−6026.

(26) Wang, S.; Li, X.; Xun, S.; Wan, X.; Wang, Z. Y. *Macromolecules* **2006**, *39*, 7502−7507.

(27) Boyer, J. H.; Haag, A. M.; Sathyamoorthi, G.; Soong, M.-L.; Thangaraj, K.; Pavlopoulos, T. G. *Heteroatom Chem.* **1993**, *4*, 39−49.

(28) Garcia-Moreno, A. C. I.; Campo, L.; Sastre, R.; Amat-Guerri, F.; Liras, M.; Lopez Arbeloa, F.; Banuelos Prieto, J.; Lopez Arbeloa, I. *J. Phys. Chem. A* **2004**, *108*, 3315−3323.

(29) Charleux, B.; Delaittre, G.; Rieger, J.; D'Agosto, F. *Macromolecules* **2012**, *45*, 6753−6765.

(30) Annotation by the author: mass of styrene, corrected by the loss of styrene by evaporation during the sonication step (25%). For each experiment, a loss of 25% of styrene has been determined by comparing gravimetric results and ^{1}H NMR spectra ($CDCl_3$, residual vinylic protons; see Figure SI-9, Supporting Information).

(31) To the best of our knowledge, the reactivity ratio for the copolymerization of styrene with phenyl acrylate have not been tabulated. We therefore determined r_S with the Kelen-Tüdös method for the copolymerization of styrene with πPhA 2 (see Figure SI-2, Supporting Information). The value for r_S was 0.37 ± 0.03.

(32) Tacx, J. C. J. R.; Ammerdorffer, J. L.; German, A. L. *Polym. Bull.* **1984**, *12*, 343−348.

(33) Otsu, T.; Ito, T.; Fukumizu, T.; Imoto, M. *Bull. Chem. Soc. Jpn.* **1966**, *39*, 2257−2260.

(34) Bisht, H. S.; Ray, S. S.; Chatterjee, A. K. *J. Polym. Sci.Part A: Polym. Chem.* **2003**, *41*, 1864−1866.

(35) Odian, G. (ed.), *Principles of polymerization*, 4th ed.; Wiley-Interscience: New York, 2004; p 476.

(36) Resch-Genger, U.; Grabolle, M.; Cavaliere-Jaricot, S.; Nitschke, R.; Nann, T. *Nat. Meth.* **2008**, *5*, 763−775.

(37) Méallet-Renault, R.; Herault, A.; Vachon, J.-J.; Pansu, R. B.; Amigoni-Gerbier, S.; Larpent, C. *Photochem. Photobiol. Sci.* **2006**, *5*, 300−310.